AGU PUBLICATIONS

Geophysical Research Letters

RESEARCH LETTER
10.1002/2016GL068383

Key Points:
- A large number of volcano-tectonic earthquakes are detected and relocated using a template matching approach
- Relocated seismicity outlines a persistent ring-shaped structure at shallow depth and a vertically elongated complex at larger depths
- Magma transfer from a deep source is evidenced by a large number of upward migrating earthquakes moving toward a shallow reservoir

Supporting Information:
- Supporting Information S1
- Data Set S1

Correspondence to:
O. Lengliné,
lengline@unistra.fr

Citation:
Lengliné, O., Z. Duputel, and V. Ferrazzini (2016), Uncovering the hidden signature of a magmatic recharge at Piton de la Fournaise volcano using small earthquakes, *Geophys. Res. Lett.*, *43*, 4255–4262, doi:10.1002/2016GL068383.

Received 23 FEB 2016
Accepted 29 MAR 2016
Accepted article online 4 APR 2016
Published online 7 MAY 2016

Uncovering the hidden signature of a magmatic recharge at Piton de la Fournaise volcano using small earthquakes

O. Lengliné[1], Z. Duputel[1], and V. Ferrazzini[2]

[1]IPGS-EOST, Université de Strasbourg/CNRS, Strasbourg, France, [2]Observatoire Volcanologique du Piton de la Fournaise, Institut de Physique du Globe de Paris, La Réunion, France

Abstract We apply a template matching method to detect and locate preeruptive earthquakes at Piton de la Fournaise volcano in 2014 and 2015. This approach enabled the detection of many events and unveiled persistent seismicity features through multiple eruptions. Shallow earthquakes define a ring-shaped structure beneath the main crater. The repetitive occurrence of events along this structure suggests that it corresponds to a preexisting zone of weakness within the edifice. We also show evidence of deep magma transfer in 2015. More than 5000 deep earthquakes define an upward migration immediately followed by the occurrence of shallow events leading to an eruption 20 days later. This suggests the creation of a hydraulic connection between the lower part of the volcanic system and a magma reservoir located near sea level. We can envisage than such replenishments of the shallow reservoir occurred in the past but were undetected because of limited deep earthquake detections.

1. Introduction

Eruptions at basaltic volcanoes are often preceded by abundant seismic activity [e.g., *Collombet et al.*, 2003]. This activity serves as one of the indicators of an impeding eruption [e.g., *Schmid et al.*, 2012]. Beyond the usefulness of seismicity rate monitoring as a short-term eruption precursor at active volcanoes, earthquakes can also help to understand volcano dynamics. Volcano-tectonic (VT) earthquakes represent brittle failures within the volcanic edifice [*McNutt and Roman*, 2015]. While these events are related to stress perturbations caused by intruding magma bodies, a clear link between the stress source and the occurrence of these earthquakes is still elusive. These events are either interpreted as a direct marker of the magma pathway [e.g., *Grandin et al.*, 2011], as distributed damage within the volcanic edifice caused by the magma chamber pressure source [e.g., *Carrier et al.*, 2015] or as result of the activation of preexisting structures already near to failure [e.g., *Rubin and Gillard*, 1998]. This poses a challenge for the interpretation of preeruptive seismicity as an indicator of magma dynamics within the volcanic edifice.

A typical limitation to decipher the actual link between the magma feeding system and the occurrence of VT events is the lack of precise observations of these latter events. Volcanoes are associated with various seismic signals (e.g., long-period events, tremor, and rockfalls), which might mask the signature of VT events if they occur in at the same time. The complexity of the seismic signals, combined with the low signal-to-noise ratio for small events, results in difficulties for both the detection and precise location of VT earthquakes. Furthermore, VT events often occur in very active swarm episodes that render the identification of each separate event difficult. In these circumstances, it is usually not possible to detect and locate earthquakes accurately during preeruptive crises.

In recent years, several innovative techniques have been applied to detect and characterize the various seismic signals. These techniques have revealed tectonic seismicity in unprecedented detail, which has led to the identification of new types of seismic phenomena. In particular, *Shelly et al.* [2006] showed that nonvolcanic tremors occurring in subduction zones are composed of swarms of low-frequency earthquakes. These previously unnoticed events were detected by using a template matching approach, where continuous seismic data streams are correlated with known seismic signals included in a template database. This processing method leads to the recovery of signals within noisy data. Similar template matching approaches were used to unveil previously undetected low magnitude earthquakes [e.g., *Gibbons and Ringdal*, 2006] or

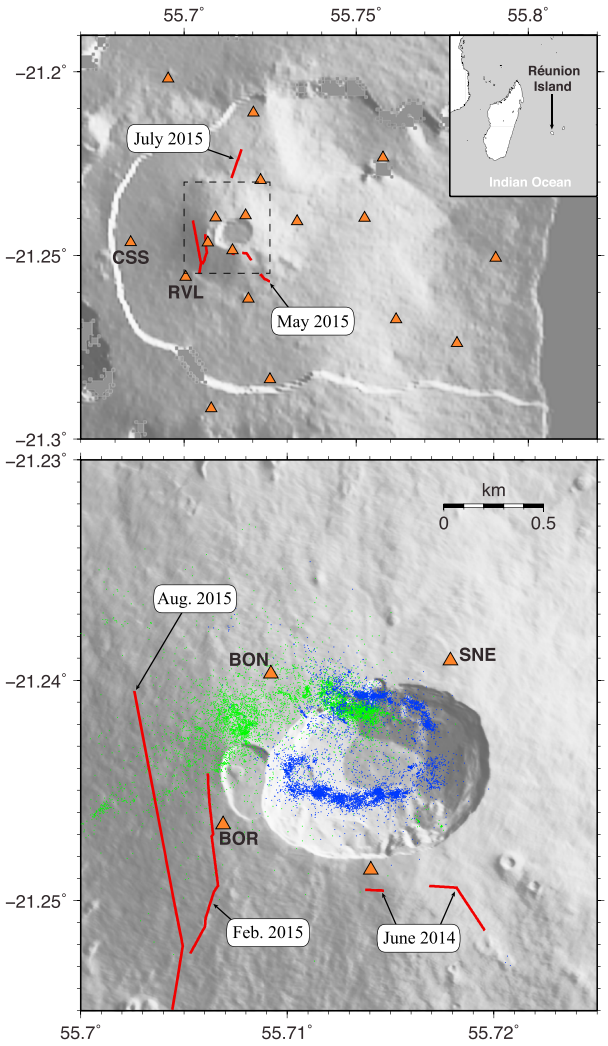

Figure 1. Volcano-tectonic setting. (top) Global map of the Piton de la Fournaise volcanic edifice. Orange triangles indicate seismic stations used in this study. Code names are indicated for stations used for event detection. The eruptive fissures of the five studied eruptions are indicated by red lines. (bottom) Same as Figure 1 (top) with the position of all relocated shallow earthquakes (blue dots) and deep events (green dots).

to uncover uncataloged seismic events following large earthquakes [e.g., *Peng and Zhao*, 2009; *Lengliné et al.*, 2012; *Shimojo et al.*, 2014].

Volcanic seismicity therefore appears as a perfect candidate for the application of this template matching technique. The recent application of this approach on Ontake volcano, Japan, revealed 30 times more events that those listed in original JMA catalog [*Zhang and Wen*, 2015]. The template matching approach can also be coupled with a relocation algorithm [e.g., *Waldhauser and Ellsworth*, 2000], such that newly detected events are then relocated relative to each other. Because of the high similarity between events, precise cross-correlation time delays can be estimated to obtain accurate relocation. *Shelly et al.* [2013a, 2013b] used such an approach to evidence migrations of seismicity that were previously undetected at Mount Rainier and Yellowstone (USA)volcanoes.

We use the template matching approach to detect events that occurred during recent eruptive unrests at Piton de la Fournaise volcano (Réunion Island, France) from June 2014 to November 2015 (see Figures 1 and S1 and Table S1 in the supporting information). Réunion Island is located in the Indian Ocean, east of Madagascar. Our approach reveals many more events than those included in the original catalog. Relocation of these newly detected events expose the structure of the volcano and highlight how the system evolves over time, in unprecedented detail. We notably resolve an upward migration of the seismicity that is interpreted

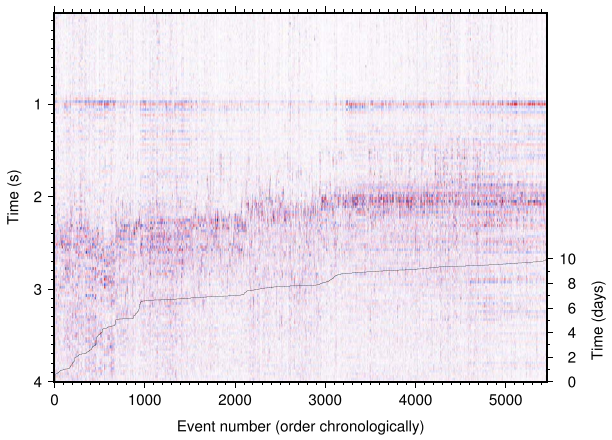

Figure 2. Vertical records at stations CSS for relocated deep events between 16 April 2015 and 25 April 2015. All waveforms are bandpass filtered between 8 and 32 Hz and normalized by their maximum amplitude. Events are ordered sequentially and are aligned on the *P* wave arrival. We can clearly see the *S* wave arrival drifting from 2.5 s for the first events to less than 2 s for the last events of the sequence. This diminution of the *S-P* arrival time attests a progressive migration of events in the direction of the station (mostly corresponding to an upward movement). The black line shows the date of occurrence of events (in days) relative to the first event of the sequence.

as a deep magma pulse recharging a shallow reservoir near sea level. This replenishment is followed by an eruption 20 days later.

2. Methods

We use continuous data recorded by 18 broadband stations of the Observatoire Volcanologique du Piton de la Fournaise (OVPF, Figure 1). All these stations are recording continuously at 100 Hz and have three components. We focus our analysis on five recent preeruptive episodes that produced abundant seismicity (listed in Table S1). A relatively small number of earthquakes were originally included in the location catalog (see Figure S1 in the supporting information). This is notably due to the fact that during periods of high seismicity rate only a small fraction of the automatically detected events can be manually picked and located. In order to detect and locate new events, we employ a template matching approach to shed new light on the nature of the volcanic seismicity at Piton de la Fournaise. The template database is built using all located events listed in the catalog during the 2014 and 2015 preeruptive seismic crises. For each template event, we extract a 5.12 s long signal starting 1 s before the *P* wave pick for all stations and on all three components. These templates are separated in two groups: (1) 680 shallow events located above sea level and (2) 73 deep events located below sea level. Waveforms are filtered in the 5–25 Hz and 8–32 Hz passband, respectively, for shallow and deep events (see Figure S3).

The earthquake detection is done using a selection of channels maximizing the signal-to-noise ratio for each group of events. For shallow events, we use the vertical components of the three summit stations (BOR, BON, and SNE). For deep events, we select the three components of CSS and RVL (cf. Figure 1). At each time step (0.01 s), we compute correlation coefficients between template waveforms and continuous records. For a given template, we obtain traces of correlation coefficients at all selected channels. We apply a maximum filter over a duration of $\pm$0.1 s and shift the correlation signal by correcting for the travel time differences between stations. We then stack the shifted correlation coefficients of all the different channels. The maximum filter allows coherent stacking even if there is a small travel time difference between the template and the detected event (i.e., if the two events are not perfectly collocated). We then set a correlation coefficient threshold to 0.4 and consider as possible detections all time windows where this threshold is exceeded. In the case where multiple templates are associated with a common detection, we simply consider one detection associated with the template giving the highest correlation coefficient. For each newly detected event, we finally extract the three component waveforms (5.12 s long) at all stations where a *P* wave pick was available in the template event. This method results in the detection of 8011 shallow earthquakes and 8049 deep events, corresponding to $\sim$10 times more shallow events and $\sim$100 times more deep events than those listed in the original catalog. A majority of the detected deep events occurred within weeks before the May 2015 eruption. Waveforms of such deep events are presented in Figure 2.

For all detected events and available channels, we compute travel time delays from cross correlation by extracting 1.28 s long time windows around the *P* and *S* wave arrivals on the vertical and the two horizontal components, respectively. On average, we extract 11 stations for *P* waves and 10 stations for *S* waves for each detected earthquake. We use a second-order polynomial fit around the maximum of the cross-correlation function to obtain subsample time delay estimates. We retain all computed time delays associated with a correlation coefficient greater than 0.7. Travel time delays are then used to infer the relative locations of

all detected events. Deep and shallow events are relocated separately since the large interevent distance between these two groups results in significant dissimilarities between waveforms (Figure 4). All newly detected events and those originally present in the catalog are all relocated together using the HypoDD software [*Waldhauser and Ellsworth*, 2000; *Waldhauser*, 2001]. For shallow events, ray parameters are computed from a homogeneous medium (straight rays). The velocity of this homogeneous medium is taken from the shallowest layer of the velocity model of the volcano: 3.5 km s^{-1}. For deep events we considered a 1-D velocity model [*Battaglia et al.*, 2005]. During the inversion process we weight similarly *P* and *S* wave travel time delays and progressively reject outliers. Events without enough links with other earthquakes are discarded at each iteration. We are able to relocate 7857 shallow events out of the 8011 detections and 6548 earthquakes out of 8049 detected deep events.

3. Results

The relocation of shallow events delineates a ring-shaped structure with a mean radius of 300 m located below the summit crater and about 700 m above sea level. The shape of this shallow structure is well constrained by relative time delay measurements, but its absolute position is uncertain as it mostly depends on the initial location of template events. Most events on this shallow structure are triggered along two east-west trending streaks (Figure 1). These two features were previously noticed by *Sapin et al.* [1996] and *Massin et al.* [2011] who interpreted them as two subvertical planes dipping toward the center of the main crater. Our results rather suggest that the vertical extent of hypocenters is much more limited and mainly results from location uncertainties. Based on earthquake relocations, we find that the seismic cloud collapses within ± 50 m of a best fitting plane (see Figure S2 in the supporting information).

Based on the spatiotemporal distribution of shallow events, we also reveal the rapid migration of earthquakes preceding several eruptions (see Figure S3 in the supporting information). Immediately before June 2014 and May 2015, the seismicity rapidly migrated along the southern cluster toward the west with a velocity of about 1.7 km h^{-1}. Such feature is also observed before February 2015 but at much lower speed (66 m h^{-1}), with a migration lasting for the entire preeruptive episode. Other migrations are visible during preeruptive swarms but are not immediately followed by an eruption. On the other hand, such temporal evolution is not visible before July 2015 and August 2015 eruptions.

All relocated deep events (below sea level) are concentrated in a small area extending mainly to the west of the two summit craters. Their location defines several structures organized in a vertically elongated complex (Figures 1 and 3). It is possible that the depth extent of seismicity partly results from uncertainties due to the trade-off between depth variation and the origin time difference of events. However, Figure 2 points out that earthquakes are progressively triggered with a diminution of the *S-P* arrival time at station CSS, located directly above these deep clusters. This shows not only that the vertical extent of seismicity is real but also that earthquakes migrates toward shallower depth with time (Figure 2). These deep earthquakes are migrating from 7.5 km to 1.5 km below sea level with longitude increasing as depth decreases. The location of these deep events coincides with the locations of the preeruptive earthquake migration identified before the 1998 eruption [*Battaglia et al.*, 2005]. Our relocations highlight a seismically quiescent zone between sea level and a depth of 1.5 km in which no earthquakes are located. The thickness of this aseismic area is not very well constrained, as it is based on the comparison of two relocated data sets (deep events and shallow events) that we process independently (see previous section). It is however in agreement with previous observations based of the seismicity at the same location [e.g., *Nercessian et al.*, 1996]

More than 80% of relocated deep events occurred between 16 and 25 April 2015. This seismicity starts at a depth of about 6 km on 16 April and seems to propagate both toward deeper and shallower depths relative to the initial location (Figure 3). The downward migration does not last more than a few days and most of the activity continues to progress upward. The seismicity reaches a depth of 2 km on 25 of April 2015 and remains active at that depth. This deep activity is then accompanied by the triggering of shallow event swarms preceding the 17 May 2015 eruption.

Although no magnitudes are computed for new detected earthquakes, they likely have lower magnitudes than the template events since they were not included in the original catalog. The largest deep template event in the catalog has a duration magnitude $M_D = 1.3$. By computing the relative amplitude between newly detected events and template events, we find that all new earthquakes (except one) have smaller amplitude,

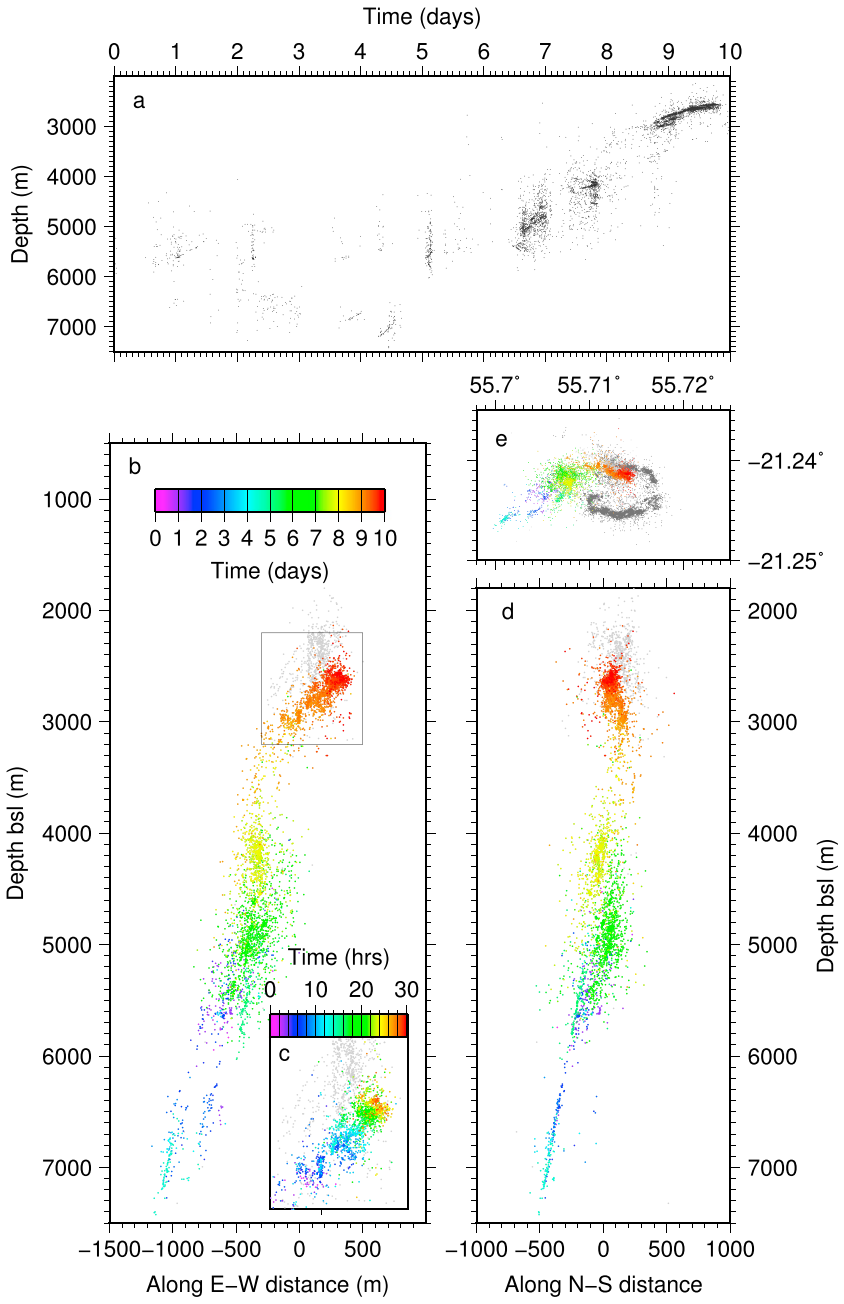

Figure 3. Spatiotemporal distribution of eathquakes. (a) Depth of seismicity as a function of time during the first 10 days of the deep seismic crisis in April 2015. The black dots represent the location of earthquakes, and the origin time is taken as 16 April 2015. The eruption started on 17 May 2015. (b) E-W and (d) N-S cross sections of the deep seismicity. The gray dots refer to the location of all deep seismic events, while colors indicate the occurrence times of those events that occurred in the first 10 days. (c) Zoom in time and space on the shallower cluster (cf. square in Figure 3b). (e) Map view of the deep seismicity migration. The gray dots correspond to relocated shallow earthquakes (plotted for reference).

which suggests that most of them have $M < 1.3$. This contrasts with the migration of seismicity resolved in 1998 where the magnitude of about 700 deep events out of a total of 3100 ranged between 1.5 and 2.2.

The vertical migration speed during this sequence is of the order of 350 m per day, which is roughly 10 times slower than the one identified preceding the 1998 eruption of the Piton de la Fournaise [*Battaglia et al.*, 2005]. Our observations also suggest that the distribution of deep events is not continuous but rather clusters at some depth intervals where intense swarms are progressively activated. The migration speed of events within these clusters is similar to the overall upward migration observed over the entire deep seismic crisis.

In the last 2 days, a west dipping bended swarm is activated between 3 km and 2 km below sea level. The migration within this cluster is not purely vertical, the events being also progressively triggered toward east (Figure 3c). The deep earthquakes occurring outside this migration sequence take place during several episodes mainly on 1, 5, and 13 May 2015 and during the last week of July 2015. During these episodes the deep seismicity is restricted to a limited depth interval between 1.5 km and 2.5 km below sea level with no apparent sign of migration.

4. Discussion and Conclusion

Our results show that the shallow preeruptive seismicity at Piton de la Fournaise occurs on some tightly clustered structures, while other areas of the volcanic edifice, including the neighborhood of the hypothetical magma pathways, remain quiet. During all of the five analyzed preeruptive periods, shallow events cluster on a persistent ring-shaped structure. The southern edge of this ring-shaped structure is associated with westward migrations of earthquakes before June 2014, February 2015, and May 2015 eruption. Since very few events are located above and below this structure, any identification of dyke propagation based on seismicity remains speculative. This could be related to our detection method, since events that are very different from templates can be difficult to recover. For example, it is possible that mode I earthquakes produced at the tip of a propagating dike are too small to be confidently picked from surface stations and thus cannot be included in the template database [*Rubin and Gillard*, 1998].

The shallow seismicity ring probably outlines preexisting zones of weakness that are triggered by static stress changes due to overpressurization of the magma chamber or dike intrusions in the volcanic edifice (probably either by shear stress increase across faults or decreased normal stress). It might correspond to a ring fault hosting repetitive collapses of the summit crater [e.g., *Staudacher*, 2010]. Such ring faults are documented in other volcanic areas [e.g., *Mori and McKee*, 1987], some of them being associated with migration of seismicity [*Prejean et al.*, 2003] or with large earthquake ruptures [*Nettles and Ekström*, 1998]. On the other hand, events being located in a very limited depth range ($\pm$50 m around a east dipping plane), we cannot totally rule out the possibility that seismicity is triggered on a single slowly slipping plane. Such slow slip process has been observed on other volcanoes [*Cervelli et al.*, 2002; *Segall et al.*, 2006] and might involve a subhorizontal detachment such as observed during the April 2007 Piton de la Fournaise eruption [*Got et al.*, 2013; *Chaput et al.*, 2014; *Froger et al.*, 2015]. To better understand the physical process driving the shallow seismicity, we are currently working on inferring focal mechanisms of shallow earthquakes. This analysis is left to a future study.

Similarly, the coincident location of upward migrating deep seismicity before March 1998 and May 2015 eruptions suggests that deep events certainly occur on persistent structures that have a low frictional strength and are near to failure. These structures might be seismically activated, as the stress source associated with an ascending magma pulse is moving through the edifice. As static stress perturbations decays rapidly with distance, the triggered activity is certainly clustered around the moving magma body but does not necessarily represent its horizontal extent. Such interpretation is consistent with the analysis of geodetic data showing an acceleration of the edifice inflation rate starting in mid-April 2015 (i.e., when the deep seismicity starts) [*Peltier et al.*, 2016]. The simultaneous increase of the CO_2/H_2O ratio in summit fumaroles also suggests enrichment in deep and likely hot fluids associated with such magma upwelling [*Peltier et al.*, 2016]. The deep seismicity migration therefore suggests the transfer of magma from a deeper source toward a shallow reservoir. This shallow magma chamber probably corresponds to the 1.5 km thick zone below sea level where no earthquakes are detected. This location agrees with the low velocity anomaly exposed by previous tomographic studies [e.g., *Nercessian et al.*, 1996; *Prôno et al.*, 2009] and with the source of deformation inverted from geodetic data for various eruptions [*Peltier et al.*, 2007, 2008, 2009, 2016]. Furthermore, the end of deep earthquake migration on 25 April 2015 is almost immediately followed by the triggering of a shallow event swarm (within half a day, Figure 4), which clearly suggests hydraulic connection across the magma chamber. The delay between the time the magma enters this reservoir on 25 April and the onset of the eruption on 17 May probably corresponds to the buildup of a sufficient pressure in order to propagate magma up to the surface.

Interestingly, we also observe the occurrence of deep events (around 2 km below sea level) following swarms of shallow earthquakes (see Figure 4 on 29 April, 13 May, 28 July, and 21 August 2015). In all these cases the onset of deep seismicity immediately follows an arrest of shallow seismic activity. A possible explanation is the difficulty of detecting deep earthquakes when shallow ones occur because they dominate the seismic

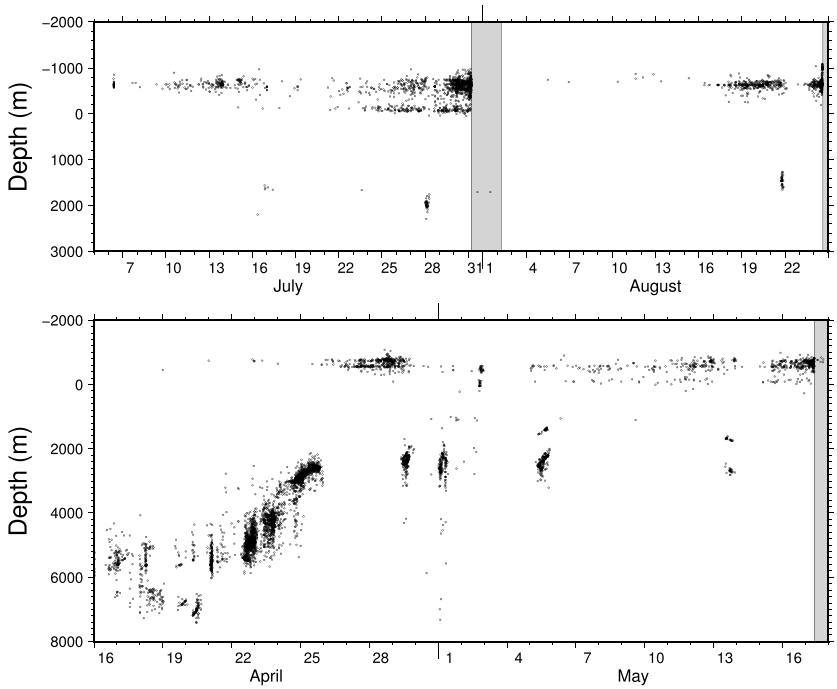

Figure 4. Evolution of earthquake depths in April–August 2015. Earthquake (black dots) depth during the preeruptive sequences of eruptions of (bottom) April–May and (top) July–August 2015. Relocated earthquakes with less than 10 travel times in total are not represented. Gray areas indicate eruption time periods.

signal. However, this possibility is unlikely as deep and shallow events are detected on two different sets of stations where they produced respectively the largest signal-to-noise ratio. These oscillations in event depths are thus probably related to variations in the position of the stress source.

Our analysis enabled the identification and location of many more events than originally included in the catalog. The template matching method is an efficient approach to recover small events when visual identification of the seismic signals and of the arrival times is difficult. In particular, it is noteworthy to realize that only 27 deep earthquakes were initially present in the catalog in April 2015, while several thousands of upward migrating events were detected in this study. We can envisage that migrations from a deep magma source, such as the one presented here, could have occurred in the past but were undetected because only a few earthquakes could be identified and located. A notable exception is the preeruptive seismicity preceding the 1998 eruption, which produced events large enough to be readily identified [*Battaglia et al.*, 2005]. One could speculate that such unnoticed deep magma transfers could provide an explanation for the occurrences of the many eruptive episodes of the Piton de la Fournaise volcano since 1998. This method could also be used to better understand preeruptive behavior at volcanoes worldwide.

Acknowledgments
We thank Patrice Boissier, Julia Cantarano, Jean-Luc Got, Robin Matoza, Aline Peltier, Benoit Taisne, Michel Tas, and Nicolas Villeneuve for helpful discussions. We thank two anonymous reviewers for suggestions. We thank Mike Heap for grammatical assistance. Data are available through the eida.ipgp.fr arclink server and at the OVPF upon request. This research was supported by the Initiative d'Excellence (IDEX) funding framework (Université de Strasbourg) and the CNRS-INSU Tellus-ALEAS program. Figures were made with the GMT software [*Wessel and Smith*, 1998].

References

Battaglia, J., V. Ferrazzini, T. Staudacher, K. Aki, and J.-L. Cheminée (2005), Pre-eruptive migration of earthquakes at the Piton de la Fournaise volcano (Réunion Island), *Geophys. J. Int.*, *161*(2), 549–558.

Carrier, A., J.-L. Got, A. Peltier, V. Ferrazzini, T. Staudacher, P. Kowalski, and P. Boissier (2015), A damage model for volcanic edifices: Implications for edifice strength, magma pressure, and eruptive processes, *J. Geophys. Res. Solid Earth*, *120*, 567–583, doi:10.1002/2014JB011485.

Cervelli, P., P. Segall, K. Johnson, M. Lisowski, and A. Miklius (2002), Sudden aseismic fault slip on the south flank of Kilauea volcano, *Nature*, *415*(6875), 1014–1018.

Chaput, M., V. Pinel, V. Famin, L. Michon, and J. L. Froger (2014), Cointrusive shear displacement by sill intrusion in a detachment: A numerical approach, *Geophys. Res. Lett.*, *41*, 1937–1943, doi:10.1002/2013GL058813.

Collombet, M., J.-R. Grasso, and V. Ferrazzini (2003), Seismicity rate before eruptions on Piton de la Fournaise volcano: Implications for eruption dynamics, *Geophys. Res. Lett.*, *30*, 2099, doi:10.1029/2003GL017494.

Froger, J. L., V. Famin, V. Cayol, A. Augier, L. Michon, and J.-F. Lénat (2015), Time-dependent displacements during and after the April 2007 eruption of Piton de la Fournaise, revealed by interferometric data, *J. Volcanol. Geotherm. Res.*, *296*, 55–68.

Gibbons, S. J., and F. Ringdal (2006), The detection of low magnitude seismic events using array-based waveform correlation, *Geophys. J. Int.*, *165*(1), 149–166.

Got, J.-L., A. Peltier, T. Staudacher, P. Kowalski, and P. Boissier (2013), Edifice strength and magma transfer modulation at Piton de la Fournaise volcano, *J. Geophys. Res. Solid Earth*, *118*, 5040–5057, doi:10.1002/jgrb.50350.

Grandin, R., et al. (2011), Seismicity during lateral dike propagation: Insights from new data in the recent Manda Hararo–Dabbahu rifting episode (Afar, Ethiopia), *Geochem. Geophys. Geosyst.*, *12*, Q0AB08, doi:10.1029/2010GC003434.

Lengliné, O., B. Enescu, Z. Peng, and K. Shiomi (2012), Decay and expansion of the early aftershock activity following the 2011, M_w9.0 Tohoku earthquake, *Geophys. Res. Lett.*, *39*, L18309, doi:10.1029/2012GL052797.

Massin, F., V. Ferrazzini, P. Bachèlery, A. Nercessian, Z. Duputel, and T. Staudacher (2011), Structures and evolution of the plumbing system of Piton de la Fournaise volcano inferred from clustering of 2007 eruptive cycle seismicity, *J. Volcanol. Geotherm. Res.*, *202*(1), 96–106.

McNutt, S. R., and D. C. Roman (2015), Chapter 59—Volcanic seismicity, in *The Encyclopedia of Volcanoes (Second Edition)*, 2nd ed., edited by H. Sigurdsson, pp. 1011–1034, Academic Press, Amsterdam, doi:10.1016/B978-0-12-385938-9.00059-6.

Mori, J., and C. McKee (1987), Outward-dipping ring-fault structure at rabaul caldera as shown by earthquake locations, *Science*, *235*(4785), 193–195.

Nercessian, A., A. Hirn, J.-C. Lépine, and M. Sapin (1996), Internal structure of Piton de la Fournaise volcano from seismic wave propagation and earthquake distribution, *J. Volcanol. Geotherm. Res.*, *70*(3), 123–143.

Nettles, M., and G. Ekström (1998), Faulting mechanism of anomalous earthquakes near Bárdarbunga Volcano, Iceland, *J. Geophys. Res.*, *103*(B8), 17,973–17,983.

Peltier, A., T. Staudacher, and P. Bachèlery (2007), Constraints on magma transfers and structures involved in the 2003 activity at Piton de La Fournaise from displacement data, *J. Geophys. Res.*, *112*, B03207, doi:10.1029/2006JB004379.

Peltier, A., V. Famin, P. Bachèlery, V. Cayol, Y. Fukushima, and T. Staudacher (2008), Cyclic magma storages and transfers at Piton de La Fournaise volcano (La Réunion hotspot) inferred from deformation and geochemical data, *Earth Planet. Sci. Lett.*, *270*(3), 180–188.

Peltier, A., P. Bachèlery, and T. Staudacher (2009), Magma transport and storage at Piton de La Fournaise (La Réunion) between 1972 and 2007: A review of geophysical and geochemical data, *J. Volcanol. Geotherm. Res.*, *184*(1), 93–108.

Peltier, A., F. Beauducel, N. Villeneuve, V. Ferrazzini, A. Di Muro, A. Aiuppa, A. Derrien, K. Jourde, and B. Taisne (2016), Deep fluid transfer evidenced by surface deformation during the 2014–2015 unrest at Piton de la Fournaise volcano, *J. Volcanol. Geotherm. Res.*, doi:10.1016/j.jvolgeores.2016.04.03.

Peng, Z., and P. Zhao (2009), Migration of early aftershocks following the 2004 Parkfield earthquake, *Nat. Geosci.*, *2*(12), 877–881.

Prejean, S., A. Stork, W. Ellsworth, D. Hill, and B. Julian (2003), High precision earthquake locations reveal seismogenic structure beneath Mammoth Mountain, California, *Geophys. Res. Lett.*, *30*, 2247, doi:10.1029/2003GL018334.

Prôno, E., J. Battaglia, V. Monteiller, J.-L. Got, and V. Ferrazzini (2009), P-wave velocity structure of Piton de la Fournaise volcano deduced from seismic data recorded between 1996 and 1999, *J. Volcanol. Geotherm. Res.*, *184*(1), 49–62.

Rubin, A. M., and D. Gillard (1998), Dike-induced earthquakes: Theoretical considerations, *J. Geophys. Res.*, *103*(B5), 10,017–10,030.

Sapin, M., A. Hirn, J.-C. Lépine, and A. Nercessian (1996), Stress, failure and fluid flow deduced from earthquakes accompanying eruptions at Piton de la Fournaise volcano, *J. Volcanol. Geotherm. Res.*, *70*(3), 145–167.

Schmid, A., J. Grasso, D. Clarke, V. Ferrazzini, P. Bachèlery, and T. Staudacher (2012), Eruption forerunners from multiparameter monitoring and application for eruptions time predictability (Piton de la Fournaise), *J. Geophys. Res.*, *117*, B11203, doi:10.1029/2012JB009167.

Segall, P., E. K. Desmarais, D. Shelly, A. Miklius, and P. Cervelli (2006), Earthquakes triggered by silent slip events on Kilauea volcano, Hawaii, *Nature*, *442*(7098), 71–74.

Shelly, D. R., G. C. Beroza, S. Ide, and S. Nakamula (2006), Low-frequency earthquakes in Shikoku, Japan, and their relationship to episodic tremor and slip, *Nature*, *442*(7099), 188–191.

Shelly, D. R., S. C. Moran, and W. A. Thelen (2013a), Evidence for fluid-triggered slip in the 2009 Mount Rainier, Washington earthquake swarm, *Geophys. Res. Lett.*, *40*, 1506–1512, doi:10.1002/grl.50354.

Shelly, D. R., D. P. Hill, F. Massin, J. Farrell, R. B. Smith, and T. Taira (2013b), A fluid-driven earthquake swarm on the margin of the Yellowstone caldera, *J. Geophys. Res. Solid Earth*, *118*, 4872–4886, doi:10.1002/jgrb.50362.

Shimojo, K., B. Enescu, Y. Yagi, and T. Takeda (2014), Fluid-driven seismicity activation in northern Nagano region after the 2011 M9.0 Tohoku-oki earthquake, *Geophys. Res. Lett.*, *41*, 7524–7531, doi:10.1002/2014GL061763.

Staudacher, T. (2010), Field observations of the 2008 summit eruption at Piton de la Fournaise (Ile de La Réunion) and implications for the 2007 Dolomieu collapse, *J. Volcanol. Geotherm. Res.*, *191*(1), 60–68.

Waldhauser, F. (2001), HypoDD—A program to compute double-difference hypocenter locations, *U.S.G.S. Open File Rep.*, 01–113.

Waldhauser, F., and W. L. Ellsworth (2000), A double-difference earthquake location algorithm: Method and application to the northern Hayward fault, California, *Bull. Seismol. Soc. Am.*, *90*(6), 1353–1368.

Wessel, P., and W. H. Smith (1998), New, improved version of generic mapping tools released, *Eos Trans. AGU*, *79*(47), 579–579.

Zhang, M., and L. Wen (2015), Earthquake characteristics before eruptions of Japan's Ontake volcano in 2007 and 2014, *Geophys. Res. Lett.*, *42*, 6982–6988, doi:10.1002/2015GL065165.